Purification, characterization and catalytic properties of human sterol 8-isomerase

W. David NES*[1], Wenxu ZHOU*, Allen L. DENNIS*, Haoxia LI*, Zhonghua JIA*, Richard A. KEITH†, Timothy M. PISER† and Stephen T. FURLONG‡

*Department of Chemistry and Biochemistry, Texas Tech University, Lubbock, TX 79409-1061, U.S.A., †Department of Neuroscience, CNS Discovery Unit, AstraZeneca Pharmaceutical Co., Wilmington, DE 19803-3245, U.S.A., and ‡Department of Molecular Science, CNS Discovery Unit, AstraZeneca Pharmaceutical Co., Wilmington, DE 19803-3245, U.S.A.

*CHO*2, encoding human sterol 8-isomerase (hSI), was introduced into plasmids pYX213 or pET23a. The resulting native protein was overexpressed in *erg*2 yeast cells and purified to apparent homogeneity. The enzyme exhibited a K_m of 50 μM and a turnover number of 0.423 s^{-1} for zymosterol, an isoelectric point of 7.70, a native molecular mass of 107000 Da and was tetrameric. The structural features of zymosterol provided optimal substrate acceptability. Biomimetic studies of acid-catalysed isomerization of zymosterol resulted in formation of cholest-8(14)-enol, whereas the enzyme-generated product was a Δ^7-sterol, suggesting absolute stereochemical control of the reaction by hSI. Using ^2H_2O and either zymosterol or cholesta-7,24-dienol as substrates, the reversibility of the reaction was confirmed by GC-MS of the deuterated products. The positional specific incorporation of deuterium at C-9α was established by a combination of ^{1}H- and ^{13}C-NMR analyses of the enzyme-generated cholesta-7,24-dienol. Kinetic analyses indicated the reaction equilibrium ($K_{eq} = 14$; $\Delta G^{o'} = -6.5$ kJ/mol) for double-bond isomerization favoured the forward direction, Δ^8 to Δ^7. Treatment of hSI with different high-energy intermediate analogues produced the following dissociation constants (K_i): emopamil (2 μM) = tamoxifen (1 μM) = tridemorph (1 μM) < 25-azacholesterol (21 μM) < ketoconazole (156 μM) < cholesterol (620 μM). The results were consistent with stereoelectronic features of isomerization and support the general model for Δ^7-sterol formation in cholesterol synthesis.

Key words: cholesterol, emopamil, isomerization reaction, lanosterol, stereochemistry.

INTRODUCTION

The transformation of lanosterol to cholesterol involves the rearrangement of the 8(9)-double bond [1,2]. Human sterol 8-isomerase (hSI; EC 5.3.3.5; also known as emopamil-binding protein) is considered to catalyse the interconversion of the Δ^8-bond to a Δ^7-bond by an antarafacial transposition of hydrogen in analogous fashion to the isomerization performed by related isomerase enzymes operating in cholesterol genesis [3,4]. Under normal metabolic conditions structure **5** (see Figure 1) is isomerized to structure **6**. The model for enzyme-mediated 8-to-7 isomerization predicts electrophilic attack of a proton associated

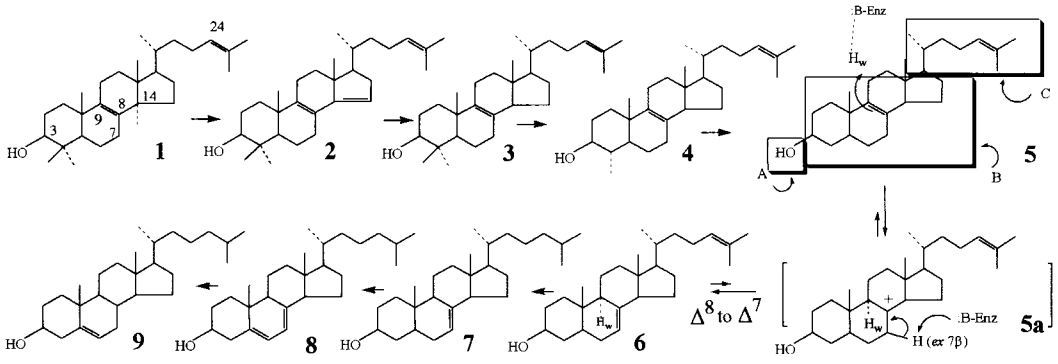

Figure 1 Hypothetical pathway of lanosterol conversion to cholesterol

Structure **5** has the three major domains for substrate recognition by the hSI. H_w^+ is the hydrogen ion in the aqueous environment and H_w is the hydrogen derived from water; only the forward reaction is shown mechanistically. **1**, Lanosterol; **2**, 4,4-dimethyl cholesta-8,14,24-trienol; **3**, 4,4-dimethyl cholesta-8,24-dienol; **4**, 4α-methyl cholesta-8,24-dienol (4α-methyl zymosterol); **5**, zymosterol; **5a**, C-8 HEI; **6**, cholesta-7,24-dienol; **7**, cholest-7-enol (lathosterol); **8**, cholesta-5,7-dienol (7-dehydrocholesterol); **9**, cholesterol. Domains of sterol recognized by the hSI are boxed in **5**.

Abbreviations used: gCOSY, gradient COSY; gHSQC, gradient heteronuclear single-quantum coherence; GPC, gel-permeation column; HEI, high-energy intermediate; HMBC, heteronuclear multiple bond correlation; hSI, human sterol 8-isomerase; MALDI-TOF MS, matrix-assisted laser-desorption ionization–time-of-flight MS; PEG, poly(ethylene glycol); RRT_c, retention time of compound relative to the retention time of cholesterol.

[1] To whom correspondence should be addressed (e-mail wdavid.nes@ttu.edu).

Table 1 Identity and amino acids at select positions for sterol 8-isomerase

GenBank accession numbers corresponding to clone sources (top to bottom): Z37986.1, X97755.1, CAA86067, AF071501.1, T51727, BAB16323, JH0488, T46871, T38129, CAA80454 and P32360.

	Clone source	Molecular mass (kDa)	pI	% Similarity (% Identity)	Amino acid 76	80	133	147
Animals	*Homo sapiens*	26.4	7.9	100 (100)	H	E	S	R
	Mus musculus	26.2	7.6	90 (78)	H	E	S	R
	Cavia porcellus	26.7	8.4	88 (73)	H	E	S	R
	Rattus norvegicus	26.7	7.3	90 (81)	H	E	S	R
Plants	*Arabidopsis thaliana*	25.1	8.8	56 (30)	H	E	S	S
	Oryza sativa	24.8	8.3	54 (35)	H	E	S	S
Fungi	*Saccharomyces cerevisiae*	24.9	5.5	25 (7)	A	N	Y	A
	Neurospora crassa	28.4	7.2	23 (6)	G	N	Y	A
	Schizosaccharomyces pombe	24.7	5.9	28 (8)	G	N	Y	A
	Magnaporthea grisea	24.7	5.8	27 (7)	E	V	Y	A
	Ustilago maydis	26.3	6.6	23 (5)	K	K	Y	A

with an active-site amino acid on a sterol substrate that results in the formation of a cationic high-energy intermediate (HEI) at C-8 [1,3]. During the reaction a proton derived ultimately from water (H_w) is added axial to the C–C double bond at C-9, and carbon-bound equatorial 7β hydrogen is eliminated to water. The overall catalysis involves a *trans* hydrogen addition-elimination reaction.

Support for this mechanism is derived from the observation that ammonium inhibitors, which are assumed to be protonated at physiological pH and possess charge resemblance to the HEI, reduce 8-to-7-isomerase activity *in vitro* and *in vivo* in spite of the fact that such inhibitors often bear little resemblance to the relevant substrates [5–7]. Some inhibitors with overlapping pharmacological properties affecting sterol 8-isomerase activity and which bind with high affinity to the hSI, have functions unrelated to their roles as sterol biosynthesis inhibitors. For instance, the anticancer drug tamoxifen binds to an oestrogen receptor in the breast but also binds to the hSI with a K_d of 3 nM [7], and it blocks uniquely at the 8-to-7-isomerase step in steroidogenesis such that in tamoxifen-treated women there is a lowering of serum cholesterol [8]. Similar ammonium analogues of predicted carbocationic intermediates have been found to inhibit other presumptive electrophilic transformations in steroidogenesis identified with the Δ^7-, Δ^{14}- and Δ^{24}-reductase enzymes [3,9], thereby providing strong support for the proposed cationic reaction mechanisms.

Numerous cDNAs of sterol 8-isomerase genes from animals, plants and fungi have been cloned and sequenced (Table 1) and in some cases functionally expressed in a yeast mutant (*erg*2) defective in sterol 8-isomerase activity [7,10]. Sequence similarity of this class of isomerase differs across evolutionary lines and amino acids considered to be associated with the topography of the active centre of the hSI, such as at position 80, are absent from their fungal counterparts [11,12]. Therefore, it is of special interest that point mutations in the human cDNA encoding sterol 8-isomerase (hereafter referred to as *CHO*2) occur naturally at positions 80, 133 and 147 [11–14]. Mutant forms E80K, S133R and R147H are responsible for lipidoses that produce an accumulation of Δ^8-sterols associated with malformations, multiple congenital anomalies, mental and growth retardations and/or skeletal and skin abnormalities, including Conradi–Hunermann or Happle (CDPX2) syndrome. Although there exists a lack of overall sequence homology of animal to fungal sterol 8-isomerases, four putative transmembrane α-helicies of potential functional significance are found in the secondary-structure predictions of the enzyme.

Studies involving mutagenesis of *CHO*2 have been performed to establish the importance of select amino acids in the protein and to establish the location of the active centre [12,14], whereas relatively little attention has been directed towards the substrate features required in binding or the mechanistic events that control the isomerization reaction. The specificity of sterol and HEI analogue are poorly defined, primarily because the hSI enzyme has not been purified and is incompletely characterized.

In this paper we describe the purification, properties and kinetic characterization of the hSI. We have used these approaches to probe the hSI catalytic reaction that involves a zymosterol–enzyme intermediate. The low abundance of sterol 8-isomerase in animal cells, which makes purification of the enzyme difficult [2], prompted us to consider an alternative strategy for generating enzyme using recombinant cDNA. Towards this goal, the sterol 8-isomerase has been overexpressed in *erg*2 yeast or BL21 (DE3) bacterial cells, purified to homogeneity and the properties of the enzyme and mechanism elucidated. By examining catalytic isomerization under different reaction conditions and studying the catalytic competence and inhibitory properties of a series of substrate mimics and HEI-type inhibitors on native hSI enzyme activity, it has been possible to establish the precise regiochemistry and stereochemistry of the hSI-promoted isomerization as well as the structural parameters of principal importance for sterol and drug in binding.

EXPERIMENTAL

Instrumentation

NMR spectroscopy of cholesta-7,24-dienol and [9-^{2}H]cholesta-7,24-dienol was carried out in [^{2}H]chloroform (600 μl) dissolved in a 5 mm NMR tube. Gradient COSY (gCOSY), TOCSY, NOESY, gradient heteronuclear single-quantum coherence (gHSQC) and heteronuclear multiple bond correlation (HMBC) spectra were recorded at 298 K with a Varian Inova 600 MHz NMR spectrometer. The TOCSY mixing time was 100 ms. NOESY spectra were recorded with mixing times of 600 ms. gCOSY and gHSQC were recorded using pulsed-field gradients for coherence selection. In a typical two-dimensional (^{1}H-^{1}H) spectrum, 512 transients of 1024 data points were recorded with a spectral width of 3200 Hz in both dimensions, and the data

were processed with zero filling to obtain a 2048 × 2048 matrix. Chemical shifts were measured relative to tetramethyl silane. ^{1}H-NMR spectra of ergosterol and other enzyme-generated products were recorded in [^{2}H]chloroform at 300 MHz (^{1}H-NMR) using a Bruker AF300 spectrometer. Chemical shifts (δ, p.p.m.) are referenced to tetramethyl silane (δ, 0) or chloroform (δ, 7.24) for ^{1}H-NMR and to chloroform (δ, 77.00) for ^{13}C-NMR. Radioactivity measurements were obtained on a Beckman LS 6500 liquid scintillation counter with 5 ml of ScintiVerse BD cocktail (Fisher) and were automatically quench-corrected. GC-MS analysis of the identification of sterols used in the enzymic reaction was with a Hewlett Packard 6890 GC interfaced to a 5973 mass spectrometer at 70 eV. GC was performed using an Agilent HP-5 column (30 m × 25 μm in diameter). Film thickness was 0.25 μm, flow rate of He was set at 1.2 ml/min, injector temperature was 250 °C, and initial column temperature was 170 °C, which was held for 1 min and increased at 20 °C/min to 280 °C.

HPLC was performed using a TSK gel C_{18} reversed-phase 25 cm analytical column (Toso Hass) eluted at room temperature with 100 % methanol at a flow rate of 1 ml/min with the detector set at 210 nm. Relative retention times in GC and HPLC are the retention times of the test sterol divided by the retention time of cholesterol (RRT_c and α_c respectively).

Substrates and reagents

[3-^{3}H]Zymosterol (14.4 mCi/mmol) was prepared from zymosterol by reduction of the 3-keto-derivative with sodium borotritide. [3-^{3}H]Cholesta-7,24-dienol (13.8 mCi/mmol) was synthesized from [3-^{3}H]zymosterol using a cell-free preparation of hSI. ^2H_2O (99 %) was purchased from Aldrich. Zymosterol and related sterols were obtained from our sterol collection [15,16]. 26-Homocholesta-8,23,26(28)-trienol was synthesized from 26,27-dehydrozymosterol using a preparation containing the recombinant sterol methyl tranferase as described in [17,18]. The Bradford protein assay kit and protein electrophoresis supplies were purchased from Bio-Rad. Isopropyl β-D-thiogalactoside was purchased from Research Products International. Reagents and chemicals used in the culture of bacteria, enzyme purification and activity assays were purchased from Sigma and Fisher unless otherwise noted.

Preparation of DNA constructs

The full-length cDNA for hSI was isolated from a human fetal brain cDNA library by PCR. Two oligonucleotides (forward, 5′-ATG ACT ACC AAC GCG GGC CCC TTG CAG-3′, and reverse, 5′-TCA GTT CTT CTT GCT CTT GGC TTT TGT-3′) were used to isolate the cDNA using thermostable DNA polymerase from *Thermus thermophilus*. The native hSI cDNA was then cloned into the pUC18 vector using the SureClone Ligation kit (Amersham Biosciences). To construct the bacterial expression vector, two primers (forward, 5′-CAT ATG ACT ACC AAC GCG GGC CCC-3′, and reverse, 5′-GGA TCC TCA TGT TCT TCT TGC TCT TGG C-3′) with terminal *Nde*I and *Bam*HI restriction sites were used to introduce these sites at the ends of the cDNA. The resulting PCR product was TA-ligated into the pCR2.1 plasmid. The introduced *Nde*I and *Bam*HI sites were then utilized, through a double restriction digestion reaction, to transfer the cDNA from the pCR2.1 plasmid into the pET23a bacterial expression vector. The use of the *Nde*I site at the 5′-end of the amplified cDNA eliminated the His_6 tag and allowed for the expression of the native hSI protein. The constructed plasmid was then transformed and expressed in *Escherichia coli* BL21 (DE3) cells (Novagen) using standard cloning procedures. For verification, the entire cDNA was sequenced using the dideoxy chain termination method and the ABI 310 automated sequencing services at Texas Tech University core facility laboratory (Texas Tech University, Lubbock, TX, U.S.A.). Our sequence matched the published sequence in the NCBI GenBank (accession no. BC001572), except for a neutral point mutation at base pair 87 (C to T), which does not change the encoded protein.

To express the hSI cDNA in yeast, the same cDNA was released from pCR2.1 by utilizing the plasmid's two flanking *Eco*RI restriction sites. The released fragment was then ligated with pYX213 (pre-cut with *Eco*RI and treated with alkaline phosphatase to prevent self-ligation). The pYX213 expression vector (Ingenius) has a *GAL1* promoter and *URA3* selection marker, which allowed for the selection of transformants on SC minimal medium lacking the uracil amino acid. Sequence-verified pYX213-hSI construct was introduced into *erg*2 yeast cells for functional complementation.

Purification of hSI protein

All manipulations were carried out at 4 °C. Expression vector pYX213-hSI was transformed into eng2 *Saccharomyces cerevisiae* (a gift from Dr Martin Bard, Indiana University-Purdue University at Indianapolis, Indianapolis, IN, U.S.A.) [10] and grown to stationary phase in YPG medium (1 % yeast extract, 2 % peptone and 2 % galactose) at 30 °C. Typical harvest yields were 10 g fresh weight/litre, yielding approx. 26 mg of partially pure hSI. Cells were pelleted by centrifugation at 1100 ***g*** and treated with zymolase to generate spheroplasts as described in [19]. The 100000 ***g*** supernatant was subjected to 4.5–12 % poly(ethylene glycol) (PEG) 3350 precipitation. The resulting 100000 ***g*** pellet was dissolved in 1 vol. of buffer A (50 mM Tris/HCl, 2 mM MgCl, 1 mM EDTA, 2 mM 2-mercaptoethanol and 5 % glycerol, pH 7.5) and loaded on to a Mono-Q HR anion-exchange column (Pharmacia 5/10). Proteins were eluted with a 150 ml linear gradient from 0 to 0.6 mM NaCl in buffer A. hSI activity eluted over a set of eight fractions corresponding to 0.25–0.35 mM salt. The eluate of the active fractions was pooled and concentrated by ultrafiltration (YM 10 membrane; Amicon) and loaded on to a gel-permeation column (GPC; Pharmacia Hiprep 26/60 Sephacryl S-300). The GPC was developed in buffer A containing 10 mM NaCl and 5 % detergent (polyxyethylene 10 tridecylether). The purified hSI activity eluted as a single peak corresponding to a molecular mass of 107000 Da, based on the mobility of protein molecular-mass standards (Bio-Rad), chromatographed on the GPC under similar conditions. Protein concentrations were determined by the Bradford method [20]. To establish the turnover number of the hSI, the protein concentration was determined at A_{280} using the extinction coefficient of 74590 $M^{-1} \cdot cm^{-1}$. Western blot, protein sequencing, gel electrophoresis and molecular mass determination were as described in [18,21].

Homogenates from *erg*2 cells

Microsomes from *erg*2 cells harbouring *CHO*2 were suspended in 1 vol. of homogenizing buffer (50 mM Tris/HCl, 2 mM $MgCl_2$, 1 mM EDTA, 2 mM, 2-mercaptoethanol, 5 % BSA and 20 % dextrose, pH 8.0) and added to liquid nitrogen. Frozen cells were ground with sea sand and the crude homogenate centrifuged at 10000 ***g*** for 30 min, and the resulting supernatant was centrifuged at 100000 ***g*** for 60 min, providing microsomal pellets used as a source of hSI. Microsomes were resuspended in 5 vol. of buffer A and stored at −20 °C. This crude enzyme

preparation could be stored at −20 °C for 2 months without significant loss of activity.

Homogenates from *E. coli* BL21 (DE3)

A single colony of *E. coli* BL21 (DE3) cells was inoculated with 1 litre of Luria broth medium (10 mg/ml Difco bacto-tryptone, 5 mg/ml Difco yeast extract and 10 mg/ml NaCl, pH 7.0) and 1 ml of ampicillin stock (at a concentration of 50 mg/ml) and incubated at 37 °C at 250 rev./min for 8–10 h to reach a *D* value of approx. 1.0 (mid-logarithmic growth phase). Then eight portions of 20 ml each were inoculated into eight 2.7 litre Fernbach flasks containing 1 litre of Luria broth medium with 50 mg/ml ampicillin and the cultures were incubated for 2 h at 250 rev./min to a *D* of 0.5 and induction was performed with isopropyl β-D-thiogalactoside (0.4 mM) at 37 °C for 3 h. The cells were harvested by centrifugation at 10000 ***g*** for 5 min. Generally, from 1 litre of medium approx. 4 g (fresh weight) of cell pellet was obtained.

A standard enzyme assay contained, in a total volume of 600 μl, 0.5 or 1 mg/ml total protein from BL21 (DE3) or *erg*2 cells, respectively, Tween-80 (1.0 %, w/v) and 50 μM zymosterol prepared in buffer A. All samples were changed to buffer A by desalting or concentration prior to assay. Incubations were performed at 37 °C with continuous shaking for 3 h at pH 7.5. The reaction was terminated with 0.5 ml of 10 % methanolic KOH. The resulting organic layer was pooled and dried under a stream of nitrogen. The residue was analysed by GC-MS.

Analysis of *erg*2 sterols

Yeast cells (0.5–2.0 g of fresh weight) were saponified in 2 ml of 10 % methanolic KOH and 2 ml of DMSO at 95 °C for 30 min. After the addition of half a volume of water, the non-saponifiable lipids were extracted three times with 3 vol. of *n*-hexane and the solvent was evaporated to dryness under a nitrogen stream. The resulting residue was dissolved in 50 μl of acetone or methanol for analysis by GC-MS or HPLC respectively. Cholesterol was used as an internal standard for the quantification of the sterols. In some cases, the sterols of the non-saponifiable lipid fraction were purified by HPLC and further analysed by ^{1}H-NMR.

Steady-state analysis

The amount of substrate conversion to product was obtained from the total-ion-current chromatograms of the GC profiles. Chromatographic peak areas corresponding to substrate and product were integrated by the software integrator (Chemstation version 3.0). Product yield (in μM) = (substrate added μM) · [peak area of product/(peak area of substrate + peak area of product)]. Percentage of conversion = (product yield/substrate added) × 100 %.

The peak areas in GC were found to be directly proportional to the mass of the sterol injected into the GC column with a S.E.M. of less than 3 %. With these chromatographic conditions, the estimated limit of detection of the enzymic activity was 0.01 nmol · min^{-1} · mg^{-1}.

In order to increase the level of sensitivity of the activity assay in the forward and reverse reactions from which the equilibrium constant could be determined, a separate set of enzyme reactions was carried out using radiotracer techniques. [3-^{3}H]Zymosterol and [3-^{3}H]cholesta-7,24-dienol were assayed with BL21 (DE3) cell preparations and the products were detected by HPLC and radioactive monitoring of the eluates. The metabolite molecules were identified by HPLC by comparison with the chromatographic mobility of authentic specimens.

Labelling experiment with ^2H_2O

PEG 3350 (2 g) was added to 10 ml of 100000 ***g*** supernatant enzyme preparation. The sample was vortexed for 1 min and incubated on ice for another 15 min. PEG-precipitated protein was collected by centrifugation at 100000 ***g*** for 30 min. The resulting pellets were dissolved into 2 ml of buffer A in which ^1H_2O was replaced by ^2H_2O. Standard assays were performed using both zymosterol and cholesta-7,24-dienol as substrates. The enzyme-catalysed deuterium-labelled products were analysed by GC-MS.

Acid-catalysed isomerization of Δ^8-sterols

To mimic the enzyme isomerization reaction, an acid-catalysed (biomimetic) isomerization was performed. Zymosterol or lanosterol (500 μg) was dissolved in 2 ml of chloroform and the solution maintained on ice for 30 min. Gaseous HCl, generated by adding concentrated sulphuric acid to NaCl, was bubbled into the solution to initiate isomerization. After 1 h the reaction was terminated by addition of concentrated NH_4OH (2 ml). The residue in the chloroform was dissolved in 500 μl of acetone, and subjected to analysis by GC-MS.

Determination of K_{eq} for isomerization

Two experiments were performed using BL21 (DE3) cells to determine the equilibrium constant (K_{eq}) of the reaction. To establish equilibrium conditions based on steady-state kinetics, the amount of protein in the activity assay was increased to 2 mg and the amount of sterol decreased to 0.8 μM [3-^{3}H]sterol. The incubation was continued for 5 h at 37 °C. The resulting [3-^{3}H]sterol mixture was isotopically diluted with 10 μg each of zymosterol and cholesta-7,24-dienol and subjected to HPLC-radiocounting analysis. In the second experiment, the K_{eq} was determined by establishing the kinetic constants (V_{max}) of the forward and backward reactions using the standard assay conditions over the concentration range 5–200 μM.

Data analysis

The initial velocity data were determined using Sigmaplot 2001 plus the Sigma enzyme kinetic program (SSPS). Measurement of $K_{m(app)}$ and $V_{max(app)}$ for sterol employed a sterol concentration range of 5–200 μM. Data were fitted to the equation:

$$v = V_{max} \cdot S/(K_m + S) \quad (1)$$

using a non-linear least-squares approach. Kinetic constants ± S.E.M. are reported in the Results section below.

Steady-state inhibitors

Kinetic analysis of competitive inhibition was done by fitting all data points to the inhibition equations based on the algorithms defined by Cleland [22] using a non-linear least-squares approach. Explicit weighting by standard errors was used for replots of derived parameters.

Competitive inhibition:

$$v = V_{max}/[1 + (K_m/S) \cdot (1 + I/K_i)] \quad (2)$$

Non-competitive inhibition:

$$v = V_{max}/[(1 + K_m/S) \cdot (1 + I/K_i)] \quad (3)$$

Uncompetitive inhibition:

$$v = V_{max}/(1 + I/K_i + K_m/S) \quad (4)$$

Free energy change of isomerization

For the minimal model of Δ^8-to-Δ^7 sterol isomerization at equilibrium:

$$A \underset{k_{-1}}{\overset{k_1}{\rightleftharpoons}} B \quad (5)$$

where Δ^8 is represented by A and Δ^7 is B. In addition,

$$k_1[A] = k_{-1}[B] \quad (6)$$

from which the equilibrium constant (K_{eq}) can by determined by measuring the product/substrate concentrations following catalysis or kinetically measuring the apparent rates of the forward and back reactions according to the equation:

$$K_{eq} = [B]/[A] = k_1/k_{-1} \quad (7)$$

The free energy change of isomerization ($\Delta G^{o\prime}$) was calculated based on the equation:

$$\Delta G^{o\prime} = -RT \cdot \ln(K_{eq}) \quad (8)$$

RESULTS

Expression of hSI in *S. cerevisiae* and *E. coli*

Because the *E. coli*-expressed hSI protein was insufficient for extensive study, we turned to the yeast system to purify hSI [23]. The enzymically active 100000 ***g*** supernatant fraction of *S. cerevisiae* harbouring *CHO*2 was found to contain ergosterol, consistent with functional complementation of the foreign gene,

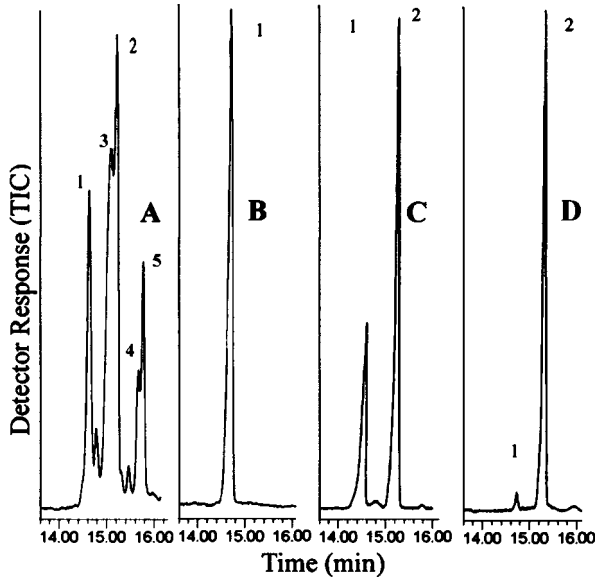

Figure 2 Total ion current (TIC) chromatograms of sterols from hSI enzyme assays performed at 37 °C for 8 h using 50 μM substrates

(**A**) Represents the non-saponifiable lipid fraction of *erg*2 microsomes harbouring the hSI cDNA assayed with zymosterol (sterol structure based on its mobility relative to the GC mobility of an authentic specimen and retention times relative to cholesterol RRT_c). TIC peak 1, zymosterol, $RRT_c = 1.2$; TIC peak 2, cholesta-7,24-dienol, 1.24; TIC peak 3, ergosterol, 1.23; TIC peak 4, ergosta-8,24(28)-dienol, 1.28; TIC peak 5, ergost-8-enol, 1.29. (**B**) Non-saponifiable lipid fraction extract of BL21 (DE3) control cell homogenate assayed with zymosterol. (**C**) Non-saponifiable lipid fraction extract of BL21 (DE3) cells harbouring hSI cDNA assayed with zymosterol. (**D**) Non-saponifiable lipid fraction extract of BL21 cells harbouring hSI cDNA assayed with cholesta-7,24-dienol.

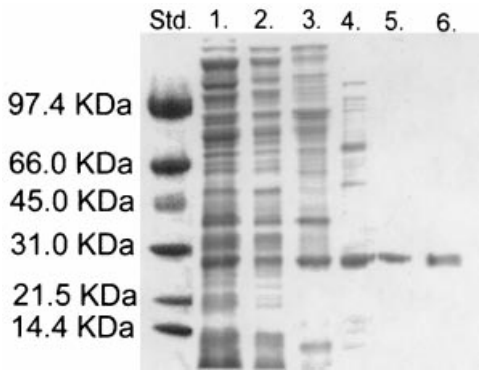

Figure 3 SDS/PAGE and immunoblot analysis of recombinant hSI expressed in *erg*2 following the purification scheme described in Table 2

Lane 1, homogenate; lane 2, 100000 ***g*** supernatant; lane 3, PEG 3350 precipitate protein fraction; lane 4, aliquot of fraction 12 from Mono-Q HR fractionation; lane 5, aliquot from the GPC fractionation corresponding to the material of 107 kDa; lane 6, Western blot of the homogenate using the anti-hSI primary antibodies as described in [18]. The gel was stained with Coomassie Brilliant Blue.

Table 2 Purification of hSI from *erg*2 cells harbouring *CHO*2

The data are based on the disruption of 10 g (fresh weight) of *erg*2 cells. Units are defined as nmol of substrate isomerized/min under the assay conditions described in the Experimental section. Recovery figures include any losses in buffer change in the preparation of the indicated step.

Fractionation step	Total protein (mg)	Total activity (units)	Specific activity (units/mg)	Recovery (%)
Homogenate	2100	11970	5.7	100
100000 ***g*** supernatant	1620	11340	7.0	94.7
PEG precipitation	440	7700	17.5	64.3
Mono Q	26.3	1066	40.6	8.9
GPC	7.0	678	243	5.6

and to generate cholesta-7,24-dienol from assay with zymosterol (Figure 2). The chromatographic [retention time of compound relative to retention time of cholesterol (RRT_c) and α_c] and spectral (MS and ^{1}H-NMR) data of ergosterol recovered from the *erg*2 cells harbouring *CHO*2 matched that of an authentic specimen [24]. In similar fashion, *E. coli* cells harbouring *CHO*2 generated cholesta-7,24-dienol from zymosterol. No hSI activity was found in BL21 (DE3) cells deficient in *CHO*2 insert and only zymosterol was recovered from the activity assay. The sterol composition of *erg*2 cells contained Δ^8-sterols (results not shown), as reported in the literature [10,11]. The apparent V_{max} of the hSI in the crude *erg*2 cell homogenate was approx. 6 nmol · min^{-1} · mg^{-1}, whereas in the crude BL21 (DE3) cell homogenate it was approx. 0.5 nmol · min^{-1} · mg^{-1}.

Purification of hSI enzyme

Using the *erg*2 cell preparation as the recombinant protein source, hSI was purified to greater than 99% purity after only three steps: (i) PEG precipitation, (ii) Mono-Q anion-exchange chromatography and (iii) gel-permeation chromatography (Figure 3, Table 2). The most active fractions containing hSI activity eluting from the Mono-Q column (Figure 4A) were concentrated by ultrafiltration to a protein concentration of 1.5 mg/ml (YM 10 membrane) and a 1 ml aliquot was subjected to gel-

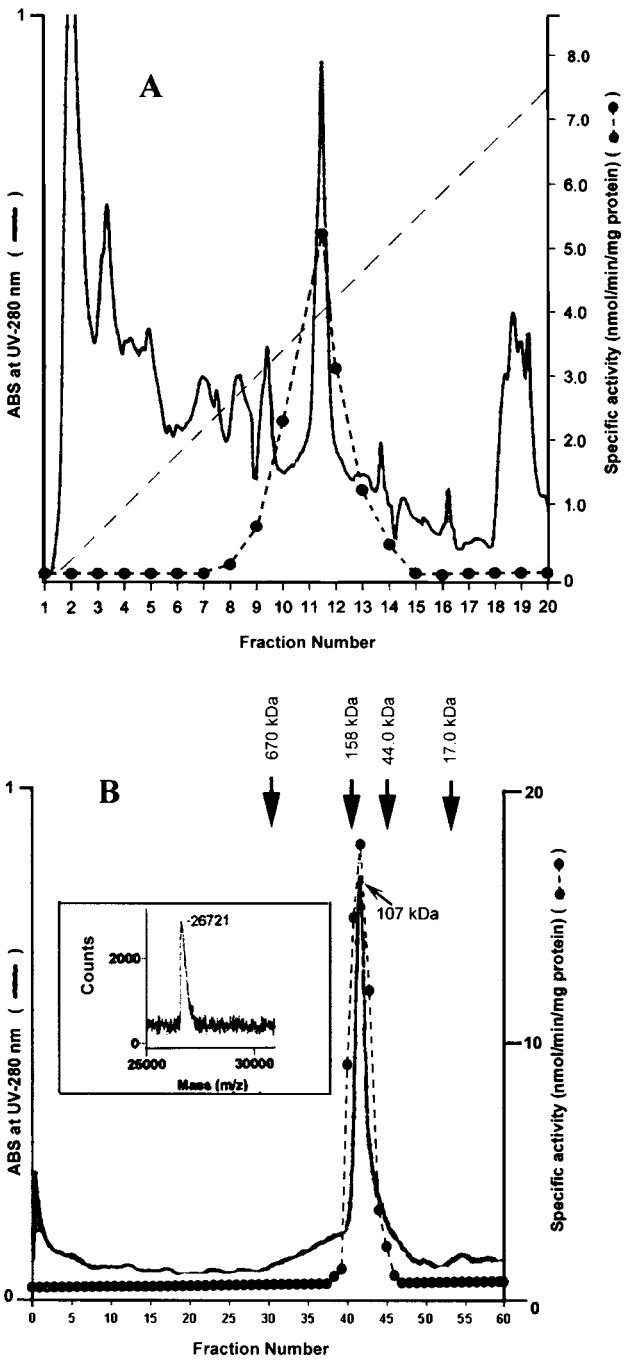

Figure 4 FPLC of hSI fractionated by Mono-Q and Sephacryl columns

Elution profile of PEG precipitates chromatographed on Mono-Q HR is shown in (**A**); 12.5 mg of PEG-precipitated protein was suspended in 5 ml of buffer A, applied to a Mono-Q HR column (2.5 cm × 30 cm) and chromatographed using a continuous gradient of buffer B (1.0 M NaCl in buffer A) added to buffer A. Sterol 8-isomerase was eluted at 0.3 mM NaCl present in the buffer. The gradient was run at a flow rate of 1.0 ml/min and 7.5 ml fractions were collected. Protein in the eluate was monitored at 280 nm. Enzyme activity (●), absorbance (solid line) and NaCl concentration (dashed line) are shown. Estimation of molecular mass of sterol 8-isomerase is shown in (**B**). Protein (1.5 mg) from Mono-Q column fractionation was loaded on a GPC Sephacryl 300 HiLoad column (2.5 cm × 60 cm) as described in the Experimental section. The molecular mass of sterol 8-isomerase was estimated to be approx. 107 kDa, eluted at fraction 43. The column was calibrated with a set of standards from Bio-Rad Laboratories (not shown is the elution of the low-molecular-mass standard vitamin B-12, which was found to elute in fraction 101). The gradient was set at a flow rate of 1 ml/min and each fraction size was 3 ml. Inset is the partial mass spectrum generated by MALDI-TOF MS showing the molecular mass of the pure hSI obtained from GPC to be approx. 26.7 kDa.

permeation chromatography on a Sephacryl 300 HiLoad column. Most of the hSI activity was associated with the main protein peak, which eluted at an apparent molecular mass of 107000 Da. Approx. 0.4 mg of pure hSI was recovered from the column (Figure 4B).

Enzyme properties

The purified protein showed a single band on SDS/PAGE with an apparent molecular mass of 27 kDa, as predicted by the complementary DNA sequence. A Western blot (Figure 3) of the purified enzyme was further support for the band migrating at approx. 27 kDa in the SDS/PAGE analysis being hSI. The protein was analysed by matrix-assisted laser-desorption ionization–time-of-flight MS (MALDI-TOF MS) and found to possess a molecular mass of 26.7 kDa, which is close to the predicted molecular mass (Table 2). The protein was submitted for molecular mass determination by Edman sequencing but no sequence was obtained, probably due to N-capping of the enzyme expressed in a eukaryote system. Further efforts were employed to digest the protein with trypsin, and a resulting peptide fragment gave the sequence YILGDNFTVC, which is identical to the first 10 amino acids at positions 111–142 resulting in the native enzyme. In buffer A, the pure recombinant enzyme had a K_m of 50 μM and a V_{max} of 243 nmol · min^{-1} · mg^{-1} for zymosterol and a catalytic-centre activity of 0.423 s^{-1}.

As a function of the expression system containing hSI, increasing amounts of homogenate protein yielded increasing rates of sterol 8-isomerase activity for zymosterol up to 0.5 or 1 mg · ml^{-1}, producing a velocity of approx. 6.0 or 0.5 nmol · min^{-1} · mg of protein^{-1} for yeast and bacterial cells, respectively, which then fell off as the protein concentration was increased. The concentration of protein was important in kinetic analyses and in establishing the forward and back reactions in terms of the equilibrium constant. The maximum activity of the over-expressed enzyme occurred at pH 7.5, which is the same for other sterol 8-isomerase enzymes [2,25].

Temperature-dependence studies on the recombinant enzyme in the range 25–50 °C indicated a bell-shaped curve of activity with the maximum activity from 35 °C to 45 °C. We chose the assay temperature of 37 °C, which corresponds to physiological temperature. Products increased with increasing time of the incubation. The rate of isomerization was linear at 50 μM zymosterol during the first 3 h of incubation in both the yeast and bacterial systems. After 6 h of incubation, the rate of isomerization did not change and the amount of cholesta-7,24-dienol formed from assay with zymosterol was approx. 90 and 70 % in the yeast and bacterial systems, respectively.

In some kinetic analyses using BL21 (DE3) cell preparations the reactions were allowed to continue overnight for approx. 8 h to maximize product accumulation. No cofactor requirements (ATP, NADP, oxygen) were found for enzyme activity, as reported for the rat liver 8-isomerase [2], but glycerol must be added to buffer A to maintain enzyme activity.

The pI of the pure protein was determined to be 7.7, which is good agreement with the predicted value for the monomer (Table 1). The molecular mass of the native protein was established by gel-permeation chromatography (Figure 4) to be 107 kDa, indicating the hSI is a tetramer of four identical subunits. In a study by Hanner et al. [26], *CHO*2 subcloned into *erg*2 cells gave a gene product in microsomal preparations with an apparent molecular mass of 27.2 kDa, and formed a functional homodimer. It appears that the correct subunit architecture of the native enzyme is as a tetramer, which agrees with the work of Paik et al. [2] on the native enzyme purified from a rat liver preparation [2].

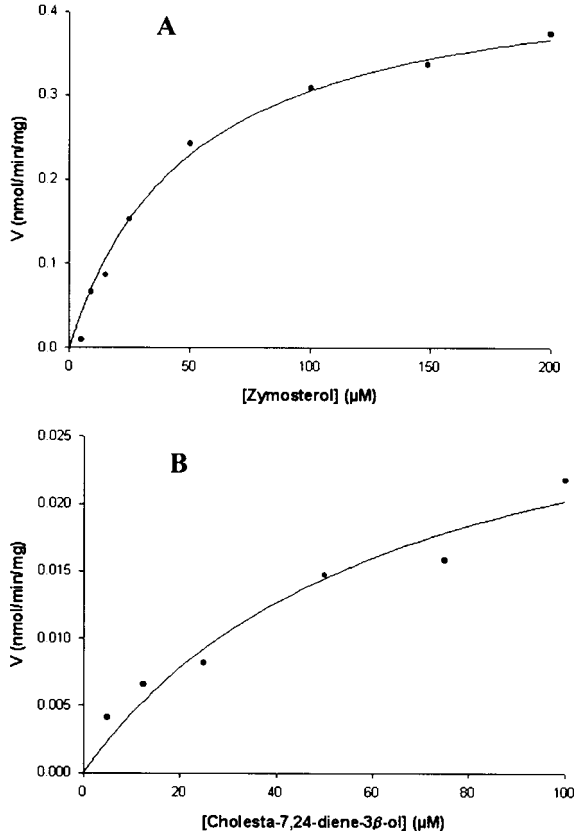

Figure 5 Michaelis–Menten hyperbolic curves of hSI using zymosterol (A) and cholesta-7,24-diene-3β-ol (B)

Homogenate of BL21 (DE3) cells harbouring *CHO2* was used for the assay at 37 °C for 3 h. The protein concentration was 1 mg/ml. 5, 15, 25, 50, 75, 100, 150 and 200 μM zymosterol were used for assays. Initial velocities were calculated based on the integration of substrate and product peak areas generated by the total ion current profiles and 5, 15, 25, 50, 75 and 100 μM ^{3}H-labelled cholesta-7,24-diene-3β-ol were used for assay and the initial velocity were obtained from the HPLC-radioactive chromatography as described in the Experimental section. Data were fitted non-linearly to the Michaelis–Menten equation using the Enzyme Kinetic Module software (SPSS; version 1.1); curves were also generated by the software, accordingly. For zymosterol, $K_m = 49.8 \pm 1.8$ μM, $V_{max} = 0.46 \pm 0.08$ nmol · min^{-1} · mg^{-1} and $r^2 = 0.97$; for cholesta-7,24-dienol, $K_m = 66.1 \pm 3.1$ μM, $V_{max} = 0.034 \pm 0.018$ nmol · min^{-1} · mg^{-1} and $r^2 = 0.95$.

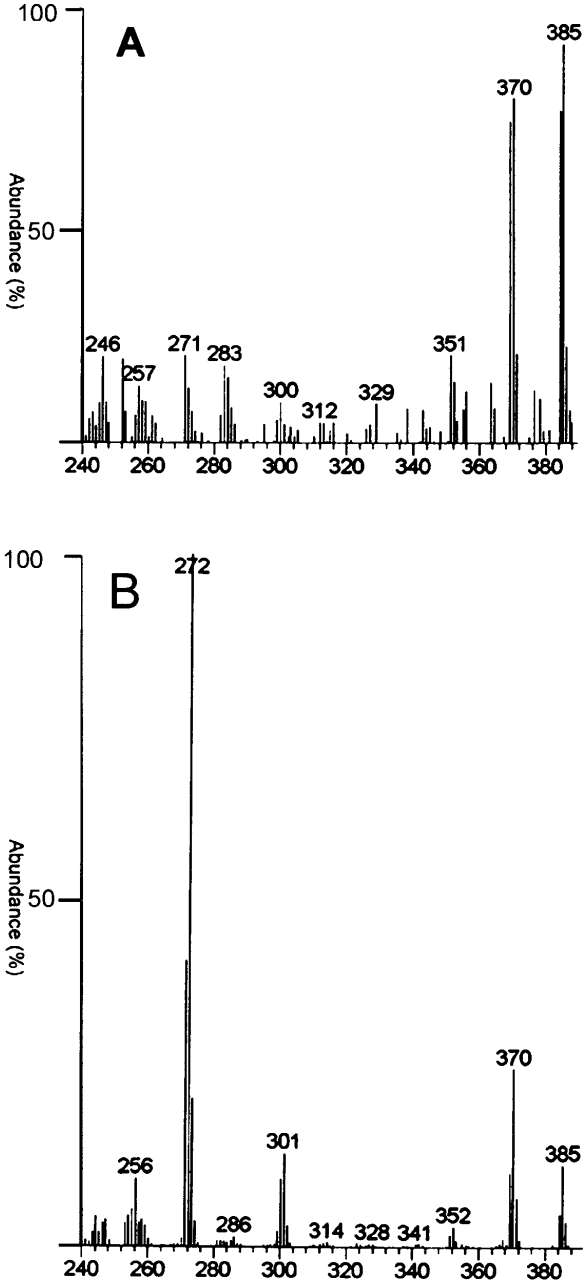

Figure 6 High-mass-end mass spectra of (A) hSI-generated [7-^{2}H]zymosterol and (B) hSI-generated [9-^{2}H]cholesta-7,24-dienol

Kinetics of the forward and reverse isomerization reactions

The initial velocity of the isomerization reaction can be determined in a straightforward manner in both the forward ([3-^{3}H]zymosterol) and reverse ([3-^{3}H]cholesta-7,24-dienol) directions using a standard assay with BL21 (DE3) cell homogenates as shown in Figure 5. The results yielded the value for $V_{max(forward)}$ of 0.46 pmol · min^{-1} · mg^{-1} and for $V_{max(reverse)}$ of 0.034 pmol · min^{-1} · mg^{-1}. The value of the equilibrium constant from eqn (7) ($K_{eq} = 13.5$) was obtained from the $V_{max(forward)}/V_{max(reverse)}$ ratio.

The value for the equilibrium constant was determined by another approach using BL21 (DE3) cells measuring the product ratios directly from the HPLC analysis after the reaction reached equilibrium. The values of K_{eq} calculated from the equilibrium experiments were 11.5 for the forward reaction and 12.5 for the reverse reaction, respectively. The K_{eq} values determined for the forward and reverse reactions by the two procedures were in reasonably close agreement and the higher value of 14 was chosen to calculate ΔG° since we can assume a somewhat better reliability in the steady-state kinetic data. The free energy of the forward isomerization was calculated to be -6.5 kJ/mol.

Labelling product with ^2H_2O

To confirm the operation of an acid–base type catalytic reaction, ^2H_2O was assayed independently with zymosterol and cholesta-7,24-dienol. The enzyme-generated products were analysed by GC-MS. The RRT_c of the deuterated product was the same as the product from control experiments assayed with ^1H_2O. However, the mass spectrum of the deuterated product (Figure 6) compared with the non-deuterated species possessed a 1 mass

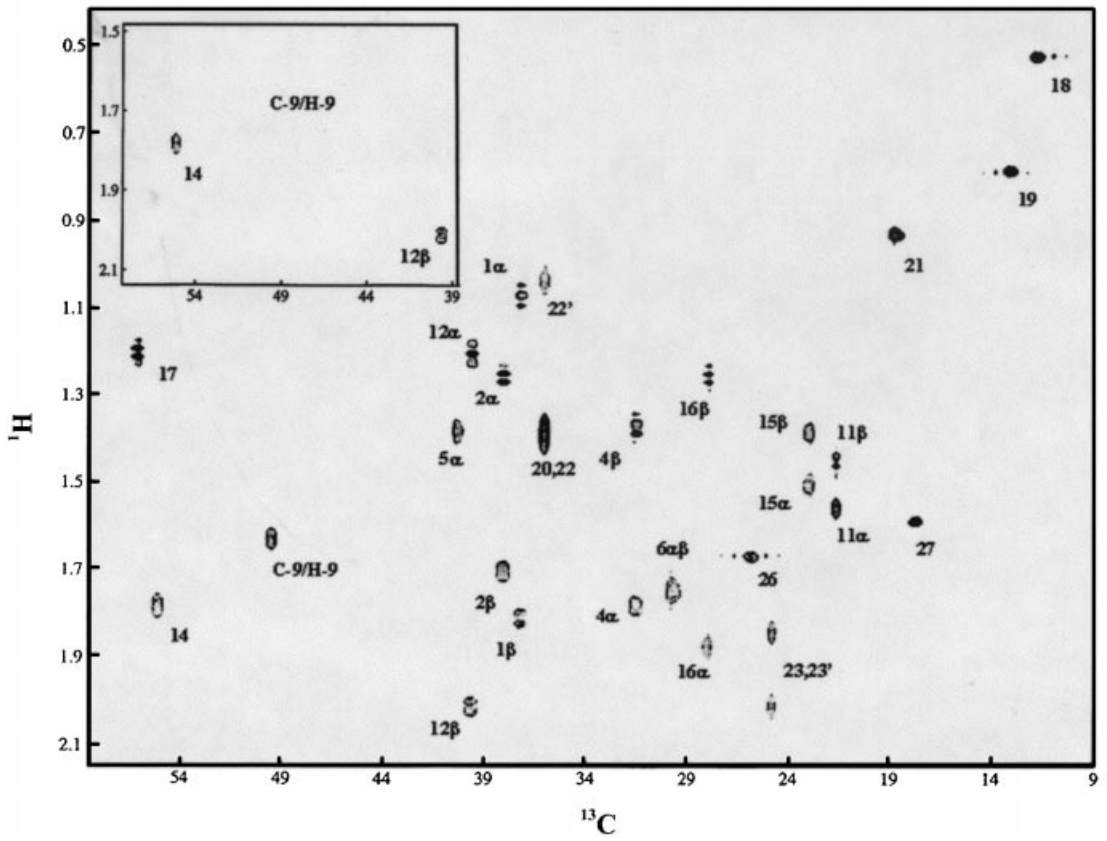

Figure 7 Two-dimensional HSQC spectrum of cholesta-7,24-dienol and partial spectrum of [9-^{2}H]cholesta-7,24-dienol (inset)

unit-higher molecular mass of $M^+ = 385$ atomic mass units, consistent with incorporation of one deuterium atom in the structure. The mass spectra of the deuterated product from the zymosterol and cholesta-7,24-dienol incubations were basically similar to the corresponding undeuterated sample except for a 1 mass unit increase in the fragmentation pattern of the deuterated sample. For mechanistic reasons (Figure 1), using zymosterol as substrate the deuterium atom originating with ^2H_2O will be introduced to position 9, producing [9-^{2}H]cholesta-7,24-dienol and using cholesta-7,24-dienol as substrate the deuterium atom will be introduced at position 7, producing [7-^{2}H]zymosterol.

Stereochemistry of [9-^{2}H]cholesta-7,24-dienol

The initial assignment of structure for the enzyme-generated cholesta-7,24-dienol and [9-^{2}H]cholesta-7,24-dienol was based on a one-dimensional 600 MHz ^{1}H- and ^{13}C-NMR analysis of the samples. The signals for individual carbon atoms matched spectra in the literature [27]. However, the signal for H-9 at δ 1.633 p.p.m. was buried under other signals in the one-dimensional ^{1}H-NMR spectrum, requiring proton mapping techniques to establish the location and stereochemistry of the H-9 atom. From gCOSY, TOCSY, gHSQC and gradient HMBC (results not shown) we were able to assign all the carbons and protons for cholesta-7,24-dienol and [9-^{2}H]cholesta-7,24-dienol. By comparison of the HSQC spectra for the two sterol samples, it was evident that C-9 was deuterated from the disappearance of the crosspeak corresponding C-9 and H-9 for the deuterium-incorporated sterol (Figure 7, inset). A weak crosspeak for C-9/H-9 appeared in the spectrum of the [9-^{2}H]cholesta-7,24-dienol, indicating that the enzyme reaction contained some traces of ^1H_2O. The stereochemistry of H-9 in cholesta-7,24-dienol juxtaposed in the α-orientation (back face of the sterol molecule) in the isomerized product was determined from NOESY between 9/1α, 9/5α and 9/12α (results not shown).

Table 3 Substrate acceptability of hSI

Activity assays were performed with BL21 (DE3) cell homogenates. Sterols shown in Figures 1 and 8 with Δ^8-bonds that are not reported in this table failed to show catalysis under the assay conditions. Structures are shown in Figures 1 and 8.

Substrate	Structure no.	Specific activity (units/mg)
Zymosterol	5	0.46
Cholest-8-enol	11	0.24
Fecosterol	10	0.11
26,27-Dehydrozymosterol	17	0.09
26-Homo-cholesta-8(9),23(24) *E*26(26′)-trienol	18	0.11
26,27-Dinorcholesta-8,24-dienol	19	0.11

Sterol specificity

The hSI was examined with a series of zymosterol substrate mimics modified in the length of the side chain, and in the geometry and electronics of key moieties present in the molecule

Table 4 Chromatographic and mass spectral data for substrates and their corresponding products generated by hSI

RRT_c is the retention time of the compound relative to the retention time of cholesterol. Numbers in parentheses are the relative mass abundance of each fragment in the spectrum. SC, side chain.

		Fragments at high-mass end of the mass spectrum			
Sterol	RRT_c	M^+	$[M-CH_3]^+$	$[M-CH_3-H_2O]^+$	$[M-SC]^+$ or $[M-SC-2H]^+$
Zymosterol	1.20	384 (100)	369 (96)	351 (2)	271 (24)
Cholesta-7,24-dienol	1.24	384 (15)	369 (28)	351 (1)	271 (100)
Cholesta-8,24(28)-dienol	1.24	398 (100)	383 (9)	365 (20)	271 (50)
Cholesta-7,24(28)-dienol	1.28	398 (6)	383 (10)	365 (3)	271 (100)
26,27-Dehydrozymosterol	1.24	382 (74)	367 (22)	349 (22)	271 (74)
26,27-Dehydrocholesta-7,24-dienol	1.27	382 (82)	367 (67)	349 (22)	271 (100)
26-Homo-cholesta-8(9),23(24) *E*,26(26′)-trienol	1.26	396 (100)	381 (78)	363 (3)	271 (62)
26-Homo-cholesta-7(8),23(24) *E*,26(26′)-trienol	1.30	396 (69)	381 (90)	363 (10)	271 (78)
26,27-Dinorcholesta-8,24-dienol	0.90	356 (100)	341 (61)	323 (16)	271 (6)
26,27-Dinorcholesta-7,24-dienol	0.93	356 (100)	341 (65)	323 (11)	271 (21)
Cholest-8-enol	1.09	386 (100)	371 (44)	353 (10)	273 (17)
Cholest-7-enol	1.12	386 (100)	371 (37)	353 (6)	273 (17)

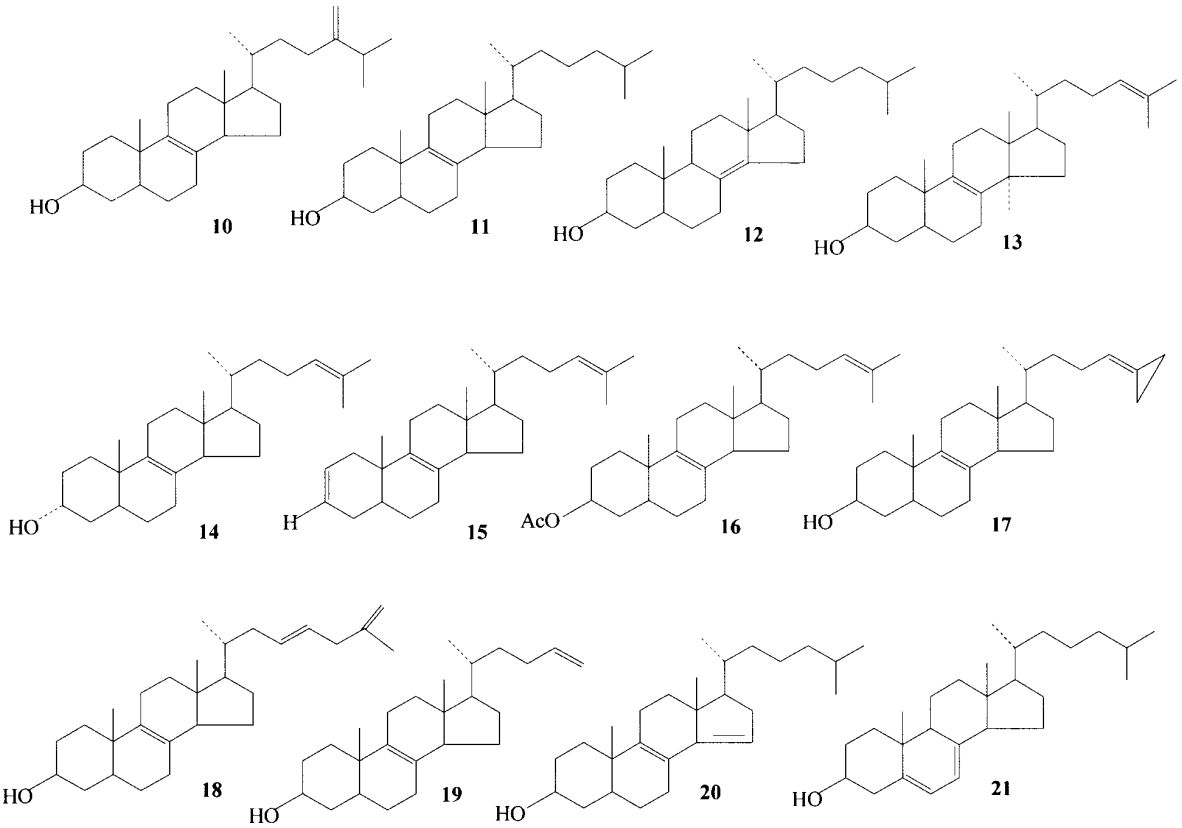

Figure 8 Structures of some sterol substrates assayed with hSI

10, Cholesta-8,24(28)-dienol (fecosterol); **11**, cholest-8(9)-enol; **12**, cholest-8(14)-enol; **13**, 14a-methyl cholesta-8,24-dienol; **14**, cholesta-8,24-dien-3α-ol (3-epizymosterol); **15**, 3-desoxy zymosterol; **16**, 3-acetyl zymosterol; **17**, 26,27-dehydrozymosterol; **18**, 26-homo-cholesta-8(9),23(24)*E*,26(26′)-trienol; **19**, 26,27-dinorcholesta-8,24-dienol; **20**, cholesta-8,14-dienol.

(Figure 7). The rate of Δ^7-sterol formation by hSI as a function of concentration of substrate was determined first, and in each case a typical hyperbolic saturation curve was obtained. The relative effectiveness of the test sterols as substrates of the hSI is reported in Table 3. GC-MS analysis of the sterol mixture following activity assay at saturating concentrations of substrates confirmed that productive binding of substrate was associated with Δ^7-product formation only (Table 4). Results for each substrate were internally consistent and expressed as the averages of multiple determinations, with V_{max} data of zymosterol analogues compared with cholesta-7,24-dienol production from zymosterol, which was used as the reference in previous studies [2,14]. The calculated K_m values for each substrate exhibiting productive binding varied within a relatively narrow range from

50 μM for zymosterol to 25 μM for, for instance, cholest-8-enol, so that catalytic parameters ($V_{relative}/K_m$) roughly paralleled the differences based on $V_{relative}$ alone. It was obvious from the structure-activity assays (Table 4) that zymosterol was the preferred substrate for Δ^7-sterol production by the hSI, followed by cholest-8-enol.

By comparing the activities of a series of alternative substrates to the activity of zymosterol (structure **5**, see Figure 1) as the reference specimen, we found the hydroxy group to be indispensable; 3-desoxyzymosterol (structure **15**, see Figure 8) is not an active substrate. By comparing zymosterol with 3-epizymosterol (structure **14**), the 3β-orientation of the hydroxyl group was demonstrated. Blockage of the hydroxyl group with an acetate group (structure **16**), demonstrated the hydroxy group must be in the free form. These findings suggest a hydrogen bond might be formed between the 3-hydroxy group and an amino acid residue in the active centre.

The enzyme can catalyse various $\Delta^{8(9)}$-sterols and Δ^7-sterols (structure **6**, Figure 1), whereas $\Delta^{8(14)}$-monoene (structure **12**, Figure 8) and $\Delta^{8,14}$-diene (structure **20**, Figure 8) structures are not bound productively. Addition of a 14α-methyl group to zymosterol (structure **13**) abolishes activity as did the addition of methyl groups to C-4 as in lanosterol (structure **1**) and 4α-methyl zymosterol (structure **4**). The presence of a double bond in the 8(14)-position most likely changes the sterol conformation thereby preventing productive binding. The presence of methyl groups at C-4 can sterically hinder the hydrogen bonding abilities of the hydroxy group at C-3. The presence of the 14α-methyl group can disturb the planarity of the back face of the sterol molecule, thereby hindering a congruous fit of the substrate in the active centre. The activity results suggest a high degree of complementarily for a flat sterol with an unhindered $\Delta^{8(9)}$-bond.

The terminal part of the side chain was also important to activity. As shown in Table 3, addition (fecosterol, structure **10**), removal (cholest-8-enol, structure **11**) or modification (26,27-dehydrozymosterol, structure **17**) of a double bond at C-24 reduces activity and lengthening (26-homo-cholesta-8,23,26-trienol, structure **18**) or shortening (26,27-dinorcholesta-8,24-dienol, structure **19**) of the side chain by one carbon atom reduces activity. These results suggest that the sterol-binding pocket recognizes three domains of the zymosterol structure, as indicated in Figure 1. The optimal sterol molecule for binding to hSI should have a C-3 equatorial hydroxy group, a planar nucleus containing a $\Delta^{8(9)}$-bond and an intact C-8 side chain containing a Δ^{24}-bond. Of the sterol features recognized by the hSI, the geometry of the C-3 hydroxy group and position of the double bond in the nucleus were most important to catalysis.

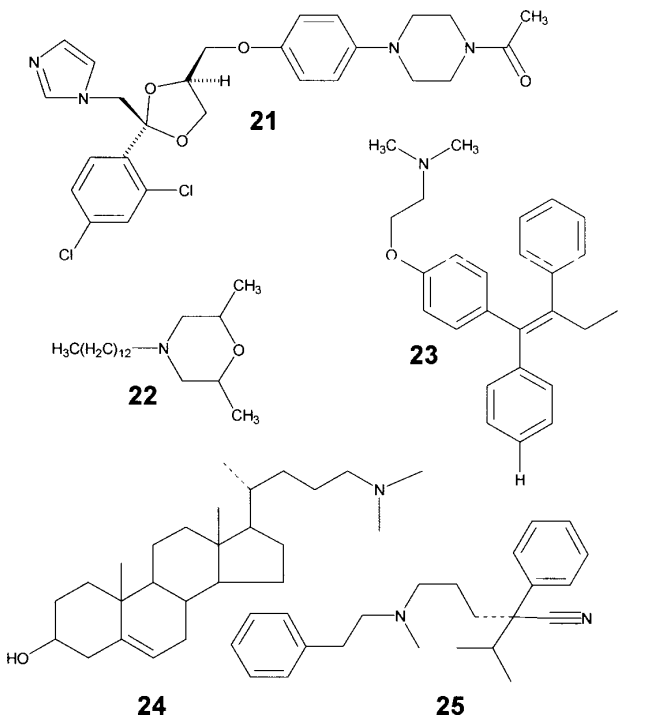

Figure 9 Structures of inhibitors assayed with hSI

21, Ketoconazole; **22**, tridemorph; **23**, tamoxifen; **24**, 25-azacholesterol; **25**, emopamil.

Table 5 Inhibitors of hSI activity

Activity assays were performed using BL21 (DE3) cell homogenates with 1 mg/ml protein at 37 °C for 3 h. The concentration of zymosterol was varied from 5 to 200 μM; the inhibitor concentration was varied between 0.5 and 5 μM or 5 and 200 μM depending on the test compound. The means of analysis and graphical methods employed for evaluating kinetic data are described in the Experimental section. Structures are shown in Figures 1 and 9.

Inhibitor	Structure	K_i (μM)
Cholesterol	9	620
25-Azacholesterol	24	21
Tridemorph	22	1
Emopamil	25	2
Tamoxifen	23	1
Ketoconazole	21	156

Effects of HEI analogues on inhibition of hSI

The general proposal for sterol 8-to-7-isomerization in cholesterol synthesis first involves α-protonation of the zymosterol substrate double bond to give an HEI, which is then converted stereoselectively to the product cholesta-7,24-dienol. Assuming the tertiary amino group of the inhibitor positions itself in the subsite of the hSI at the point normally taken up by C-8 of the zymosterol substrate, any change in the inhibitor activity found with the different HEI analogues must then be due to a difference in structure at other parts of the molecule, thereby affecting the binding mode of the HEI. With this mechanism in mind, the binding of five putative HEI analogues of sterol 8-isomerase activity (Figure 9) as well as cholesterol, a possible allosteric effector, has been examined. Inhibition kinetics were determined by Lineweaver–Burk analysis, since both the magnitude of inhibition and any possible differences in inhibition type amongst the inhibitors could be established.

By examining the pair of sterols, cholesterol and 25-azacholesterol, yielding K_i values of 620 and 21 μM respectively, it was confirmed that HEI analogues of hSI activity function with an ammonium group. Table 5 provides a summary of the data and Figure 10 illustrates a typical data set, in this instance for emopamil (structure **25**, see Figure 9), assayed over the standard zymosterol concentration range of 5–200 μM. Four HEI analogues were good inhibitors of hSI with K_i values in the range 1–21 μM and a fifth HEI analogue (structure **21**) showing minimal inhibitor potency with a K_i value of 156 μM. Kinetic plots with zymosterol, hSI and emopamil showed competitive-type inhibition by the inhibitor against the substrate, suggesting that the inhibitor binds to the same active centre as the sterol ligand. None of the inhibitors exhibited time-dependent inhibi-

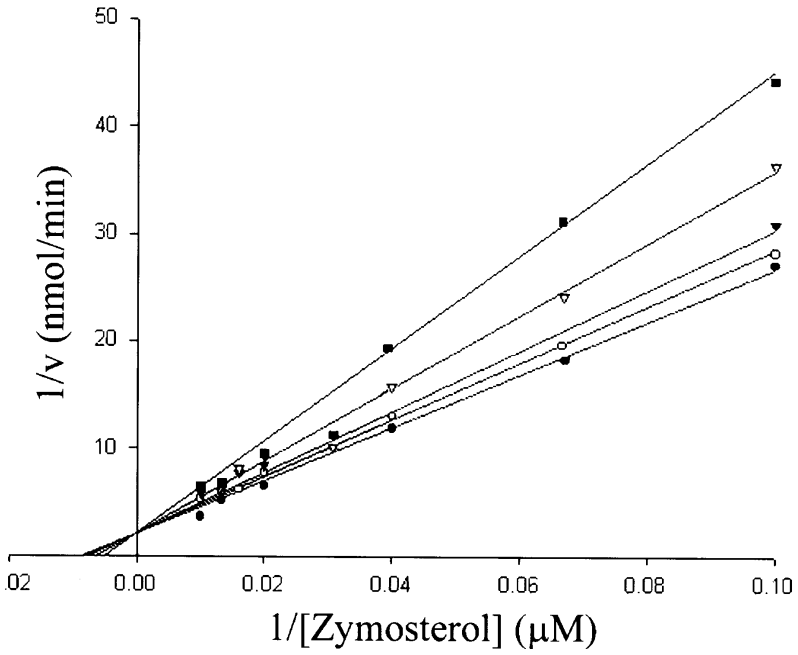

Figure 10 Double-reciprocal plot of the inhibition of hSI from BL21 cells by emopamil

hSI was assayed at 5, 25, 50, 75 and 100 μM zymosterol using the standard conditions described in the Experimental section in the presence of 0 (●), 0.1 (○), 0.2 (▼), 0.5 (▽) and 1.0 μM (■) emopamil. Curves were generated from data that were weighted as described in the Experimental section.

tion of activity, proving that they do not involve covalent modification of the enzyme to achieve inhibition. Similar competitive-type kinetic patterns were observed with cholesterol (structure **9**), 25-azacholesterol (structure **24**), ketoconazole (structure **21**), tridemorph (structure **22**) and tamoxifen (structure **23**; results not shown). Compared with tridemorph, emopamil and tamoxifen, which bind tightly to the enzyme (K_i values of 1–2 μM), ketoconazole and 25-azacholesterol bound poorly (K_i values of 156 and 21 μM respectively). No apparent relationship exists between the structure of the inhibitor or the position of the nitrogen group in the molecule and inhibitor potency, suggesting that the active centre must be quite tolerant in terms of the variety of structures accommodated. The relative binding affinities of these inhibitors indicate a distinct hydrophobic subsite for drug binding that extends in the active centre away from critical residues that provide for a productive substrate–enzyme complex, confirming related studies [6]. Notable in the case of cholesterol (structure **9**) modulation of hSI activity is the weak inhibition of hSI activity by the membrane insert. Lanosterol over the concentration range 1–200 μM could not inhibit zymosterol conversion to cholesta-7,24-dienol, consistent with the fact that lanosterol does not bind productively with the enzyme. Thus neither the first nor last sterol of the lanosterol–cholesterol pathway serve as modulators to significantly regulate carbon flux through the step controlling isomerization of the 8(9)-bond in zymosterol.

Biomimetic studies on isomerization

The product distribution after HCl-promoted isomerization of lanosterol and zymosterol was very different but chemically predictable. Thus in the case of lanosterol, since there is no C-14 hydrogen, isomerization should proceed from $\Delta^{8(9)}$ to the $\Delta^{7(8)}$ position. Alternatively, in the case of zymosterol, the 8(14) sterol should be the major product of the acid treatment because of the higher stability of the ternary carbocation C-14 versus secondary C-7. Consistent with expectation, treating lanosterol with acid, the amount of Δ^7-sterol produced is high, approx. 30 %, with no 8(14)-sterol detected in the sterol mixture. Alternatively, treating zymosterol with acid, the amount of Δ^7-sterol produced is trace, whereas the amount of 8(14)-sterol produced is high, approx. 50 % of the sterol mixture. These chemical results contrast dramatically with the sterol specificity results related to the performance of the hSI reaction using lanosterol and zymosterol as substrates, suggesting that the hSI enzyme has been subjected to natural selection as a result of evolutionary pressures on the organisms that contain the protein. The catalytic effectiveness of the hSI has clearly evolved to maximize sterol fitness to generate specific products. In view of the lack of productive binding of lanosterol and cholesterol to hSI, it seems that the ordering of the hSI enzyme in the cholesterol pathway is to sustain flux between control points.

Search for an amino acid involved with catalysis

To shed light on possible amino acid residues that contribute to catalytic isomerization, a pH-versus-log K_{cat} profile was determined of hSI assayed in phosphate buffer, as shown in Figure 11. The pK_a values for isomerization of free enzyme are centred on 6.2 and 8.7.

DISCUSSION

Recombinant hSI protein yields in the yeast system were 5–10 times the yield from expression in BL21 (DE3) cells. Expression of the native and mutant hSI enzyme in yeast cells has been

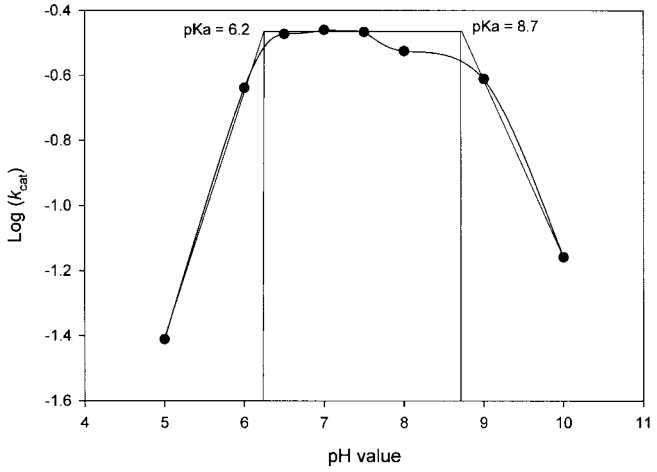

Figure 11 A pH versus log K_{cat} profile of sterol 8-isomerase

A linear regression is illustrated indicating points of convergence at pH 6.6 and 8.7.

accomplished to confirm the identity of the gene by functional complementation, to establish kinetic constants, $K_{m(zymosterol)} = 25\ \mu M$ and $V_{max(zymosterol)} = 0.325\ nmol \cdot min^{-1} \cdot mg^{-1}$, of the enzyme and to determine the functional significance of mutations introduced into *CHO2* [6,14]. However, as noted by Moebius et al. [14], it is technically demanding to characterize the *in vitro* properties of the enzyme. First, the substrate, zymosterol, is not commercially available. Secondly, large amounts of microsomal protein are required to obtain even minimal kinetic constants and even then there is a concern because the apparent V_{max} of the substrate is extremely low, making sterol specificity tests difficult. Thirdly, the substrate concentration cannot be increased arbitrarily because the solubility of zymosterol is limited. Finally, hSI is a membrane-bound protein [24]; as a result its purification can be very difficult [2].

In our studies of hSI we overcame many of the problems discussed above. Preparative amounts of zymosterol and the other sterols were synthesized for testing. *E. coli* was found to be useful as an expression system because the bacteria can make adequate amounts of hSI for some kinetic analyses of the enzyme and it does not possess a sterol enzymic pathway [28]. We therefore could introduce the *CHO2* gene into *E. coli* and study several enzyme parameters fairly quickly with crude homogenates without sterol contamination, a problem encountered using microsomal preparations of yeast [14]. *S. cerevisiae* was found to be useful as an expression system to generate large amounts of protein for characterization. The recombinant protein could be overexpressed in the 100000 ***g*** supernatant, making its purification straightforward. The problem of solubility of sterol was not a concern in the steady-state analyses since in determining K_m values we could examine a substrate concentration range of 5–200 μM.

The biomimetic studies, taken together with the structure-activity studies involving hSI, confirm the importance of regiochemistry in hSI-promoted isomerization and suggest that the native pathway for cholesterol synthesis operates under physiological conditions, as shown in Figure 1. A lanosterol–cholesterol pathway involving 8(14)-sterols [29] seems unlikely. Detection of sterols, such as 24,25-dihydrolanosterol, cholest-8-enol or cholesta-5,24-dienol (desmosterol) [3,4] signify aberrant biochemistry in the human cells. These sterols can arise from either drug treatment or a change in cholesterol homoeostasis. Such changes will affect the processing and accumulation of intermediates in the pathway, thereby limiting cholesterol production and generating disease. The finding that the hSI has a rather broad specificity for nitrogen-containing drugs can be a concern for treatment of some diseases and is reason to consider rationally designed mechanism-based inactivators of hSI, as considered for the inactivation of sterol methyl transferase [18].

The general picture which emerges from these studies is one in which the binding–isomerization of zymosterol is stereospecific. The positional specific incorporation of deuterium during catalytic isomerization proceeds as predicted by the mechanism to C-9α [1]. From the limited information on catalytic-centre activities of pure enzymes that act on sterols k_{cat} data are reported for human sterol 8-isomerase 0.423 s^{-1} (this study) and for 14α-demethylase from rat is 0.24 s^{-1} [30]. The activity of pure enzymes from the lanosterol-ergosterol pathway of *S. cerevisiae* act even slower than the enzymes from the cholesterol pathway with catalytic-centre activities for the sterol methyl transferase of 0.01 s^{-1} [18] and for 14α-demethylase of 0.003 s^{-1} [31]. The slow activity of enzymes in the post-squalene sterol pathway is likely related to the primary function of sterol end products as architectural component of membranes. Since the rates of specific enzymes in the sterol pathway in yeast and man can differ, and that key enzymes in the ergosterol pathway in yeast may be absent from the cholesterol pathway in man (e.g., the sterol methyl transferase), suggests these differences may be exploited for rational drug design.

The data presented here are consistent with a general acid-base mechanism for sterol 8-isomerization that involves zymosterol as the preferred substrate for the hSI. Plausible candidates for the immediate proton acceptor based on the pH versus log K_{cat} profiles would be a water molecule, a deprotonated imidazole group of a histidine residue, a thiol group of cysteine or an N-terminal amino group (pK_a values for the three amino residues = 6.5–8.5) [32]. Indeed, consistent with our analysis (Table 1 and Figure 11) and the report by Moebius et al. [14] on alanine screening of hSI, His^{76} (Table 1) appears to be a possible critical residue in the active centre in promoting isomerization.

The remarkable stereochemical control in the formation of a Δ^7-sterol from zymosterol shows a tight fit of substrate in the sterol–enzyme complex and is entirely consistent with the general stereochemical model for catalysis of zymosterol to form cholesta-7,24-dienol [1,5,9]. Inhibition studies with HEI analogues indicated that there is a separate subsite for the inhibitors in the active centre and confirmed that a carbocationic reaction intermediate is formed during conversion of zymosterol to cholesta-7,24-dienol. The free energy of isomerization shows the system is not at equilibrium when zymosterol and cholesta-7,24-dienol are both at their presumed physiological concentrations (approx. 50 μM, based on their K_m values); in fact, the forward reaction is favoured under these conditions because ΔG^o is negative (-6.5 kJ/mol). Therefore the equilibrium must lie to the right, with a higher concentration of zymosterol than cholesta-7,24-dienol. Studies with sterol analogues indicated for the zymosterol substrate that the C-3 hydroxy group was the principal determinant of substrate recognition and C-24-C-25 olefin was recognized largely on the basis of side-chain length whereas the primary basis for interaction with the C-8-C-9-olefin was electronic.

We thank Mr Jialin Liu for the preparation of [3-^{3}H]zymosterol. The 600 MHz NMR analyses were recorded using an instrument at the University of Georgia Complex Carbohydrate Research Center. This work was supported by grants to W.D.N. from

AstraZeneca Pharmaceutical Co., the Welch Foundation (D-1276) and National Institutes of Health (GM63477).

REFERENCES

1 Akhtar, M., Rahimtula, A. D. and Wilton, D. C. (1970) The stereochemistry of hydrogen elimination from C-7 in cholesterol and ergosterol biosynthesis. Biochem. J. **117**, 539–542
2 Paik, Y. K., Billheimer, J. T., Magolda, R. L. and Gaylor, J. L. (1986) Microsomal enzymes of cholesterol biosynthesis from lanosterol. Solubilization and purification of steroid 8-isomerase. J. Biol. Chem. **261**, 6470–6477
3 Myant, N. B. (1981) The Biology of Cholesterol and Related Steroids, Heinemann Medical Books, London
4 Popjak, G. (1986) Biosynthesis of cholesterol and related substances. In Lipids: Chemistry, Biochemistry, and Nutrition (Mead, J. F., Alfin-Slater, R. B., Howtwon, D. R. and Popjak, G., eds.), pp. 350–354, Plenum Press, New York
5 Baloch, R. I. and Mercer, E. I. (1987) Inhibition of sterol Δ^8- to Δ^7-isomerase and Δ^{14}-reductase by fenpropimorph, tridemorph and fenpropidin in cell-free enzyme systems from *Saccharomyces cerevisiae*. Phytochemistry **26**, 663–668
6 Moebius, F. F., Reiter, R. J., Bermoser, K., Glossmann, H., Cho, S. Y. and Paik, Y. K. (1998) Pharmacological analysis of sterol Δ^8,Δ^7 isomerase proteins with [^{3}H]ifenprodil. Mol. Pharmacol. **54**, 591–598
7 Paul, R., Silve, S., De Nys, N., Dupuy, P. H., Bouteiller, C. L., Rosenfeld, J., Ferrara, P., Le Fur, G., Casellas, P. and Loison, G. (1998) Both the immunosuppressant SR31747 and the antiestrogen tamoxifen bind to an emopamil-insensitive site of mammalian Δ^8,Δ^7 sterol isomerase. J. Pharmacol. Exp. Ther. **285**, 1296–1302
8 Gylling, H., Pyrhonen, S., Mantyla, E., Maenpaa, H., Kangas, L. and Miettinen, T. A. (1995) Tamoxifen and toremifene lower serum cholesterol by inhibition of Δ^8-cholesterol conversion to lathosterol in women with breast cancer. J. Clin. Oncol. **13**, 2900–2905
9 Rahier, A. and Taton, M. (1997) Fungicides as tools in studying postsqualene sterol synthesis in plants. Pest. Biochem. Physiol. **57**, 1–27
10 Ashman, W. H., Barbuch, R. J., Ulbright, C. E., Jarrett, H. W. and Bard, M. (1991) Cloning and disruption of the yeast C-8 sterol isomerase gene. Lipids **26**, 628–632
11 Braverman, N., Lin, P., Moebius, F. F., Obie, C., Moser, A., Glossmann, H., Wilcox, W. R., Rimoin, D. L., Smith, M. and Kratz, L. et al. (1999) Mutations in the gene encoding 3β-hydroxysteroid-Δ^8,Δ^7-isomerase cause X-linked dominant Conradi-Hunermann syndrome. Nat. Genet. **22**, 291–294
12 Derry, J. M., Gormally, E., Means, G. D., Zhao, W., Meindl, A., Kelley, R. I., Boyd, Y. and Herman, G. E. (1999) Mutations in a Δ^8-Δ^7 sterol isomerase in the tattered mouse and X-linked dominant chondrodysplasia punctata. Nat. Genet. **22**, 2862–2890
13 Herman, G. E. (2000) X-Linked dominant disorders of cholesterol biosynthesis in man and mouse. Biochim. Biophys. Acta **1529**, 357–373
14 Moebius, F. F., Soellner, K. E., Fiechtner, B., Huck, C. W., Bonn, G. and Glossmann, H. (1999) Histidine77, glutamic acid81, glutamic acid123, threonine126, asparagine194, and tryptophan197 of the human emopamil binding protein are required for *in vivo* sterol Δ^8-Δ^7 isomerization. Biochemistry **38**, 1119–1127
15 Venkatramesh, M., Guo, D. A., Jia, Z. and Nes, W. D. (1996) Mechanism and structural requirements for transformation of substrates by the (S)-adenosyl-L-methionine:$\Delta^{24(25)}$-sterol methyl transferase from *Saccharomyces cerevisiae*. Biochim. Biophys. Acta **1299**, 313–324
16 Nes, W. D., Janssen, G. G. and Bergenstrahle, A. (1991) Structural requirements for transformation of substrates by the (S)-adenosyl-L-methionine:$\Delta^{24(25)}$-sterol methyl transferase. J. Biol. Chem. **266**, 15202–15212
17 Nes, W. D. (2000) Sterol methyl transferase: enzymology and inhibition. Biochim. Biophys. Acta **1529**, 63–88
18 Nes, W. D., McCourt, B. S., Zhou, W. X., Ma, J., Marshall, J. A., Peek, L. A. and Brennan, M. (1998) Overexpression, purification, and stereochemical studies of the recombinant (S)-adenosyl-L-methionine: $\Delta^{24(25)}$- to $\Delta^{24(28)}$-sterol methyl transferase enzyme from *Saccharomyces cerevisiae*. Arch. Biochem. Biophys. **353**, 297–311
19 Ausubel, F. M. (1995) *Saccharomyces cerevisiae*. In Short Protocols in Molecular Biology: a Compendium of Methods from Current Protocols in Molecular Biology (Ausubel, F., Brent, R., Kingston, R. E., Moore, D. D., Seidman, J. G., Smith, J. A. and Struhl, K., eds.), pp. 13–45, Wiley, New York
20 Bradford, M. M. (1976) A rapid and sensitive method for the quantitation of microgram quantities of protein utilizing the principle of protein-dye binding. Anal. Biochem. **72**, 248–254
21 Laemmli, U. K. (1970) Cleavage of structural proteins during the assembly of the head of bacteriophage T4. Nature (London) **227**, 680–685
22 Cleland, W. W. (1979) Statistical analysis of enzyme kinetic data. Methods Enzymol. **63**, 103–138
23 Silve, S., Dupuy, P. H., Labit-Lebouteiller, C., Kaghad, M., Chalon, P., Rahier, A., Taton, M., Lupker, J., Shire, D. and Loison, G. (1996) Emopamil-binding protein, a mammalian protein that binds a series of structurally diverse neuroprotective agents, exhibits Δ^8,Δ^7 sterol isomerase activity in yeast. J. Biol. Chem. **271**, 22434–22440
24 Venkatramesh, M. and Nes, W. D. (1995) Novel sterol transformations promoted by *Saccharomyces cerevisiae* strain GL7: evidence for 9β, 19-cyclopropyl to 9(11)-isomerization and for 14-demethylation to 8(14)-sterols. Arch. Biochem. Biophys. **324**, 189–199
25 Kang, M. K., Kim, C. K., Johng, T. N. and Paik, Y. K. (1995) Cholesterol biosynthesis from lanosterol: regulation and purification of rat hepatic sterol 8-isomerase. J. Biochem. (Tokyo) **117**, 819–823
26 Hanner, M., Moebius, F. F., Weber, F., Grabner, M., Striessnig, J. and Glossmann, H. (1995) Phenylalkylamine Ca^{2+} antagonist binding protein. Molecular cloning, tissue distribution, and heterologous expression. J. Biol. Chem. **270**, 7551–7557
27 Goad, L. J. and Akihisa, T. (1997) Physical data of selected sterols and triterpenes. In Analysis of Sterols, pp. 275–410, Blackie Academic Press & Professional, London
28 Nes, W. R., Adler, J. H., Frasinel, C., Nes, W. D., Young, M. and Joseph, J. M. (1980) The independence of photosynthesis and aerobiosis from sterol biosynthesis in bacteria. Phytochemistry **19**, 1439–1443
29 Ruan, B., Wilson, W. K., Pang, J., Gerst, N., Pinkerton, F. D., Tsai, J., Kelley, R. I., Whitby, F. G., Milewicz, D. M., Garbern, J. and Schroepfer, Jr, G. J. (2001) Sterols in blood of normal and Smith-Lemli-Opitz subjects. J. Lipid Res. **42**, 799–812
30 Nitahara, Y., Aoyama, Y., Horiuchi, T., Noshiro, M. and Yoshida, Y. (1999) Purification and characterization of rat sterol 14-demethylase P450 (CYP51) expressed in *Escherichia coli*. J. Biochem. (Tokyo) **126**, 927–933
31 Lamb, D. C., Kelly, D. E., Venkateswarlu, K., Manning, N. J., Bligh, H. F., Schunck, W. H. and Kelly, S. L. (1999) Generation of a complete, soluble, and catalytically active sterol 14 α-demethylase-reductase complex. Biochemistry **38**, 8733–8738
32 Mathews, C. K. and Van Holde, K. E. (1995) in Biochemistry (Mathews, C. K., van Holde, K. E. and Ahern, K. G., eds.), 2nd edn, p. 131, Benjamin/Cummings Publishing Co., Menlo Park, CA

Received 5 April 2002/21 June 2002; accepted 19 July 2002
Published as BJ Immediate Publication 19 July 2002, DOI 10.1042/BJ20020551